Neoplasma 2023; 70(6): 777–786

doi:10.4149/neo_2023_230103N4

CHAC1 promotes cell ferroptosis and enhances radiation sensitivity in thyroid carcinoma

Xinlin YANG[1,#], Miao ZHANG[2,#], Wei XIA[1], Zhongchao MAI[1], Ying YE[2], Bin ZHAO[3,*], Yanan SONG[2,*]

[1]Department of Nuclear Medicine, The Seventh People's Hospital, Shanghai University of Traditional Chinese Medicine, Shanghai, China; [2]Central Laboratory, The Seventh People's Hospital, Shanghai University of Traditional Chinese Medicine, Shanghai, China; [3]General Surgery Department, The Seventh People's Hospital, Shanghai University of Traditional Chinese Medicine, Shanghai, China

**Correspondence: zhaobin0727@sina.com; ynsongh7@126.com*
[#]Contributed equally to this work.

Received January 3, 2023 / Accepted November 29, 2023

ChaC glutathione-specific γ-glutamylcyclotransferase 1 (CHAC1) is involved in intracellular glutathione depletion, ferroptosis, and tumorigenesis. The functional role of CHAC1 expression in thyroid carcinoma has not yet been established. The present study aimed to investigate the impact and mechanisms of CHAC1 on ferroptosis and radiation sensitivity in thyroid carcinoma. CHAC1 expression was examined in tumor tissue specimens and microarrays and thyroid carcinoma cell lines. CHAC1 was silenced or overexpressed by lentivirus transfection in thyroid carcinoma cells. Cell viability and lipid ROS levels were evaluated by Cell Counting Kit-8 and flow cytometry, respectively. The effect of CHAC1 on tumor growth *in vivo* was also measured. Ferroptosis-related proteins were measured by western blotting. CHAC1 expression was decreased in patients with thyroid carcinoma, and overexpression of CHAC1 suppressed cell viability of BCPAP cells and tumor growth in xenografted nude mice. Exposure to Ferrostatin-1, a ferroptosis inhibitor, significantly attenuated the inhibitory effects of CHAC1 overexpression on cell viability. In CHAC1-overexpressing BCPAP cells, ferroptosis was induced as indicated by increased lipid ROS production and PTGS2 expression. Knocking down of CHAC1 in K1 cells significantly induced cell viability, reduced lipid ROS production and PTGS2 expression, and enhanced GPX4 expression. Such effects were attenuated by RSL3, a ferroptosis inducer. Furthermore, we showed that CHAC1 overexpression enhanced radiation sensitivity in BCPAP cells as indicated by decreased cell viability, while CHAC1 knockdown had reversed effects in K1 cells as indicated by increased cell viability. Taken together, CHAC1 overexpression promoted ferroptosis and enhanced radiation sensitivity in thyroid carcinoma.

Key words: thyroid carcinoma; CHAC1; ferroptosis; GPX4

Thyroid carcinoma is the most prevalent cancer in the endocrine system, accounting for approximately 95% of all endocrine tumors [1]. The incidence of thyroid carcinoma has been steadily rising in the world over the past 30 years [2, 3]. Thyroid carcinoma can be categorized into papillary, follicular, medullary, and anaplastic subtypes based on histological characteristics [1]. Papillary thyroid carcinoma and follicular thyroid carcinoma are the two most comment types of thyroid carcinoma [4]. Patients with thyroid carcinoma have a relatively favorable prognosis after surgical resection and radiotherapy as compared to other types of cancer [5]. However, tumor recurrence is the main reason for patients with advanced thyroid carcinoma. Therefore, it is urgently needed to explore the molecular mechanisms of thyroid carcinoma development.

Ferroptosis, a newly discovered form of regulated cell death in recent years, has been investigated in cancer and cancer treatment [6]. Iron dependence is a distinguishing feature of ferroptosis [7, 8]. During ferroptosis, decreased cellular glutathione levels lead to the accumulation of lipid reactive oxygen species (ROS) and ultimately cause cell death [9]. Ferroptosis is characterized by increased lipid ROS, smaller mitochondria, increased mitochondrial membrane density, and decreased mitochondrial crest [10]. Several intracellular signaling molecules and signaling pathways, such as glutathione peroxidase 4 (GPX4), cystine-glutamate antiporter (System Xc-), and

p62-Keap1-NRF2 pathway, have been suggested to mediate this process through regulating glutathione levels [9].

ChaC glutathione-specific γ-glutamylcyclotransferase 1 (CHAC1) is a member of the ChaC family of γ-glutamylcyclotransferases (γ-GCTs) [11]. CHAC1 has a structure (BtrG/γ-GCT fold) and an active site similar to γ-GCT and mediates the degradation of cellular glutathione [12]. Knockout of the CHAC1 gene resulted in embryonic lethality, suggesting that CHAC1 is an important intracellular functional regulator [13]. Overexpression of CHAC1 led to intracellular glutathione depletion and increased ROS levels, and decreased GPX4 protein levels [14]. Growing evidence linked CHAC1 to tumorigenesis. The expression of CHAC1 was closely related to the prognosis of breast and ovarian cancer [15, 16]. Chen et al. reported that CHAC1 overexpression in human triple-negative breast cancer cells may result in high levels of oxidative stress and ferroptosis by increasing GSH degradation [17]. CHAC1 expression was reduced in glioma cells, and the CHAC1-Notch3 pathway was involved in the antitumor drug temozolomide-induced glioma cytotoxicity [18]. CHAC1 suppressed cell proliferation and promoted cell apoptosis in head and neck squamous cell carcinoma cells treated with nisin [19]. However, its expression and potential roles in thyroid carcinoma have not been explored.

In the current study, we elucidated the anti-tumor role of CHAC1 overexpression in thyroid carcinoma cells *in vitro* and *in vivo* and found that CHAC1 overexpression induced ferroptosis and enhanced the radiotherapy sensitivity. Additionally, protein expression of CHAC1 was negatively correlated with GPX4 in thyroid carcinoma tissues.

Patients and methods

Data source and bioinformatics analysis. The expression levels of CHAC1, GPX4, and PTGS2 in thyroid carcinoma tissues were analyzed using the University of Alabama at Birmingham Cancer (UALCAN; ualcan.path.uab.edu/). The prognostic value of CHAC1, GPX4, and PTGS2 and the correlation between CHAC1 and GPX4 or PTGS2 in thyroid carcinoma samples were evaluated using analysis tools of Gene Expression Profiling Interactive Analysis (GEPIA). Moreover, 60 thyroid carcinoma and 10 normal thyroid tissue microarrays were purchased from Outdo BioTech.

Immunohistochemistry (IHC) analysis. Thyroid carcinoma tissue microarrays were subjected to IHC analysis. After deparaffinization and blocking of endogenous peroxidases, 0.01 M citrate sodium buffer solution (pH 6.0) was applied to the sections at 100 °C for 10 min to perform the antigen retrieval. Subsequently, endogenous peroxidase was quenched with 0.3% H_2O_2, and non-specific binding was eliminated by 10% bovine serum albumin (BSA). Then, the sections were incubated with primary antibodies against CHAC1 (diluted in 1:100; Abcam; ab279365) at 4 °C overnight. The sections were incubated with HRP-conjugated rabbit secondary antibody at room temperature for 1 h, developed with DAB substrate, and counterstained with hematoxylin. Immunoreactivity was scored using the H-score system as previously described [20]. Patients were separated into the high- or the low-expression group (cutoff point of H-score = 6).

Cell culture and treatment. Thyroid carcinoma cell lines, K1, BCPAP, and TPC1 cells, and a normal human thyroid follicular epithelial cell line, Nthy-ori3-1 (Cell Bank of Shanghai Biology Institute, Chinese Academy of Science, Shanghai, China) were cultured in RPMI-1640 medium (Biosharp) supplemented with 10% fetal bovine serum (Invitrogen) at 37 °C with 5% CO_2. Cells were treated with Ferrostatin-1 (Fer-1; SML0583; Sigma), RSL3 (IR1120; Solarbio), 3-methyladenine (3-MA; IM0190; Solarbio), Z-VAD-FMK (IZ0050; Solarbio), or vehicle (DMSO) for 48 h. Irradiation was applied with 6 MV energy and at a 2 Gy/min. The radiation was performed via a Varian linear accelerator (Varian Medical Systems, Palo Alto, CA, USA) with different doses (2, 4, 6, and 8 Gy) for 48 h.

Lentivirus preparation. Short hairpin RNA (shRNA) oligos targeting CHAC1 (shCHAC1-1, 5'-CCAAGATGCTCCTGACCAA-3'; shCHAC1-2, 5'-CCAAGGAGGTCACCTTCTA-3'; shCHAC1-3, 5'-GACGCTCCTTGAAGATCAT-3') and control shRNA (shNC, 5'-GGACGAGCTGTACAAGTAA-3') were annealed and cloned into the pLKO.1 construct (Addgene, Cambridge, MA, USA). The constructs, along with packaging plasmids, psPAX2 and pMD2.G, were transfected into 293T cells with Lipofectamine 2000 (Invitrogen) according to the manufacturer's protocol. After 48 h, a virus-containing medium was collected. K1 cells were transduced with a construct expressing CHAC1 shRNA or control shNC vector by using Lipofectamine 2000 Reagent following the instructions of the manufacturer.

CHAC1 overexpression. To overexpress CHAC1, the full-length human CHAC1 was cloned into the pcDNA3.1 construct (Life Technology). BCPAP cells were transfected with a construct expressing CHAC1 or blank vector by using Lipofectamine 2000 reagent following the instructions of the manufacturer.

Quantitative real-time PCR (RT-qPCR). The TRIzol method was used to extract RNA from thyroid carcinoma cell lines and cDNA was reversed by a cDNA reverse transcription reagent kit (Takara, Japan; RR047A). We performed RT-qPCR on an ABI 7500 fast machine (Applied Biosystems, USA) using the SYBR Premix EX Taq kit. The primer sequences were listed as follows: CHAC1-F: 5'-TACAGCCGCCGTTTCTGG-3', CHAC1-R: 5'-GGCAATGGCCTCTTCAGG-3'; β-actin-F: 5'-TGTGACGTGGACATCCGCAAAG-3', β-actin-R: 5'-TGGAAGGTGGACAGCGAGGC-3'. Normalized gene expression was determined by using the $2^{-\Delta\Delta CT}$ method.

Western blot analysis. Cells or tissues were lysed in radioimmunoprecipitation buffer containing proteinase inhibitor (Beyotime) in accordance with the manufacturer's instructions. Equal amounts of protein were separated

by sodium dodecyl sulfate-polyacrylamide gel electrophoresis and transferred to nitrocellulose membranes (Millipore). After blocking with 5% skim milk, the membranes were incubated with primary antibodies at 4 °C overnight following the manufacturer's instruction. After incubation with HRP-conjugated secondary antibody (Beyotime) at room temperature for 1 h, the signal was detected with an enhanced chemiluminescence system (ECL) (Millipore). The primary antibodies were as follows: antibodies against CHAC1 (ab217808), GPX4 (ab125066), PTGS2 (ab283574), and b-actin (ab8226) were obtained from Abcam.

Cell viability assay. Cell viability was analyzed using a Cell Counting Kit-8 (CCK-8) Assay Kit (SAB). The cells cultured in 96-well plates (100 µl/well) were treated as indicated, and then 10 µl CCK-8 reagent was applied to each well. After 3 h of incubation at 37 °C with 5% CO_2 in darkness, the optical density at 450 nm (OD450) was measured using a microplate reader.

Lipid peroxidation assay with flow cytometry. The BODIPY 581/591 C11 kit (D3861, ThermoFisher Scientific) was used to measure lipid peroxidation levels. After treatment, cells were washed three times with PBS, stained with BODIPY™ 581/591 C11 fluorescent probe (10 mM final concentration), and stored at 37 °C in the dark for 10 min. Fluorescence intensity was measured at a fixed of different wavelengths between excitation/emission of 488/510 nm and excitation/emission of 488/510 nm by CytoFLEX flow cytometry (Beckman). The ratio of the emission fluorescence intensities at 590 nm to 510 nm gives the read-out for lipid peroxidation in cells.

Xenograft mouse model. The scheme of animal experiments was approved by the Animal Care Committee of The Seventh People's Hospital (approval number 2023-AR-011). Six-week-old nude mice (weighed 20–25 g) were obtained from Ziyuan Laboratory Animal Co. Ltd (Hangzhou, China). The nude mice were randomly divided into two groups (n=6/group), and then BCPAP cells transfected with CHAC1 expressing vector or blank vector were subcutaneously injected into nude mice at 5×10^6 cells/mouse. Tumor volume was measured every three days for 35 days with the following formula: volume = 1/2 × (largest diameter) × (smallest diameter)^2. At day 35, the mice were sacrificed and the weight of each xenograft was examined. The xenografts were collected, and processed for immunofluorescence staining with anti-Ki-67 (ab243878, Abcam) and western blotting assays.

Statistical analysis. Data from the three independent experiments are expressed as the mean ± standard deviation, unless otherwise described. GraphPad Prism software (version 8.4.2) was used for statistical analysis. Unpaired Student's t-test and one-way ANOVA followed by Dunnett's multiple comparisons test were used to assess the statistical significance of differences between two groups and among multiple groups, respectively. A p-value less than 0.05 was considered significant.

Results

CHAC1 expression was decreased in thyroid carcinoma tissues and cell lines. CHAC1 was significantly decreased in thyroid carcinoma tissues compared with normal thyroid tissues in UALCAN database (Supplementary Figure S1A), and GEPIA showed that the CHAC1 mRNA expression was not significantly correlated with the prognosis of patients with thyroid carcinoma (Supplementary Figure S1B). IHC staining for CHAC1 was performed in thyroid carcinoma tissue microarrays. As shown in Figures 1A and 1B, CHAC1 protein expression was decreased in thyroid carcinoma tissues in thyroid carcinoma tissues compared with normal thyroid tissues. In thyroid carcinoma tissue microarray, the high protein expression of CHAC1 was associated with a favorable prognosis (Figure 1C). Furthermore, the protein expression of CHAC1 was notably correlated with two of the clinicopathologic characteristics, tumor size, and TNM stage in the patients with thyroid carcinoma (Table 1). To study the biological effects of CHAC1 in thyroid carcinoma, we measured CHAC1 mRNA and protein expression levels in three thyroid carcinoma cell lines. CHAC1 mRNA and protein expression were reduced in all thyroid carcinoma cell lines compared to normal human thyroid follicular epithelial cell line (Nthy-ori3-1) (Figures 1D, 1E).

Overexpression of CHAC1 inhibited cell viability and promoted ferroptosis in thyroid carcinoma. We then overexpressed CHAC1 in BCPAP cells which had low CHAC1 mRNA and protein expression (Figures 2A, 2B). CCK-8 assay showed that CHAC1 overexpression signifi-

Table 1. Relationship between CHAC1 expression and patients' features in human thyroid carcinoma.

Parameters	CHAC1 expression		p-value
	Low (n=37)	High (n=23)	
Age (years)			0.193
<55	23	18	
≥55	14	5	
Gender			0.394
Male	17	8	
Female	20	15	
TNM stage			0.015
T1–T2	19	19	
T3–T4	18	4	
Tumor size			0.020
<3 cm	16	17	
≥3 cm	21	6	
Lymph node metastasis			0.753
No	21	14	
Yes	16	9	
GPX4 expression			0.009
Low	10	14	
High	27	9	

Note: differences between groups were done by the Chi-square test

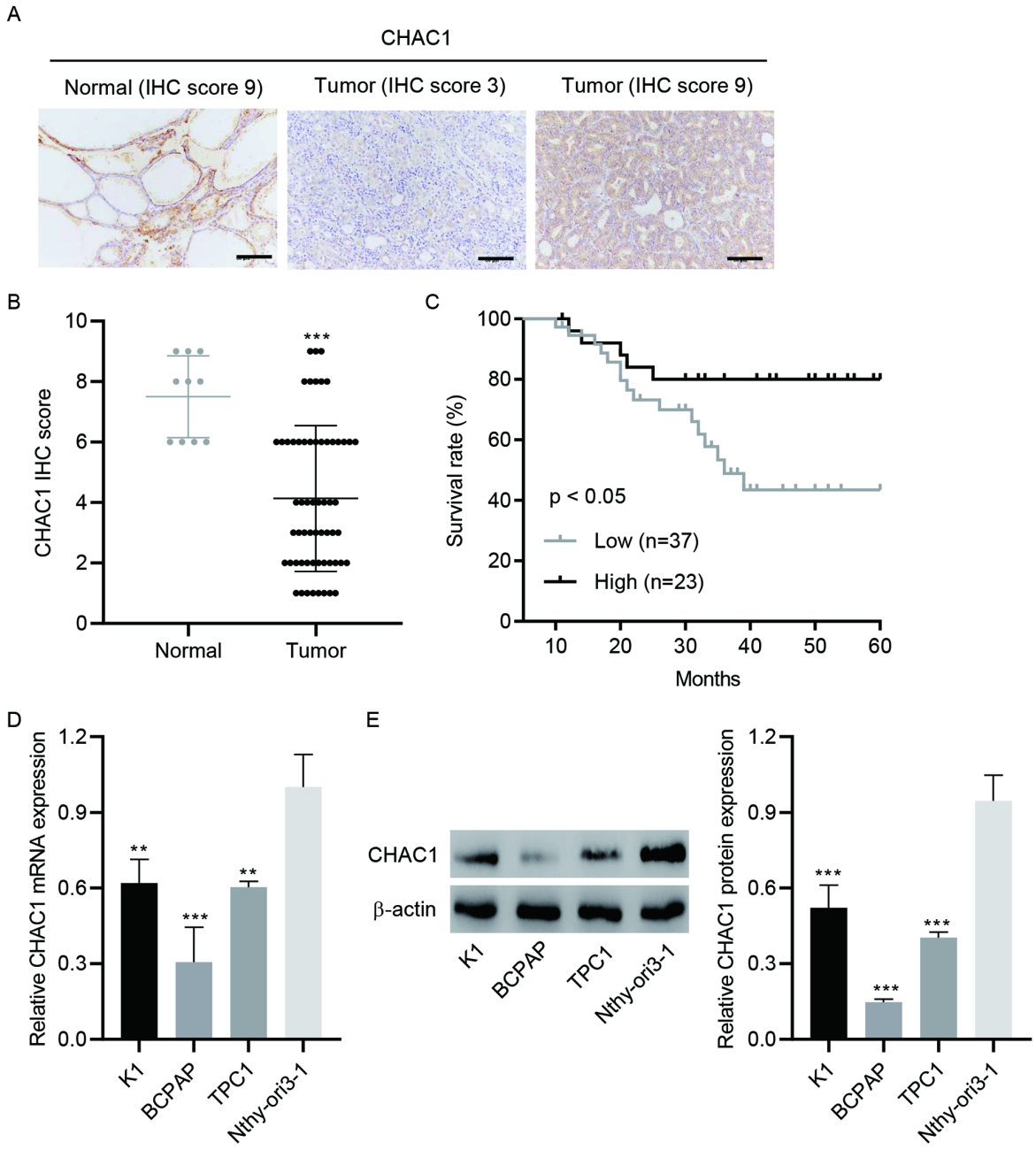

Figure 1. CHAC1 is decreased in thyroid carcinoma and cell lines. A) Box plots of CHAC1 expression in normal tissue and thyroid carcinoma tissues in the UALCAN database. B) IHC staining for CHAC1 in thyroid carcinoma tissue microarray. Scale bar, 100 mm. C) Survival analysis of patients with high and low CHAC1 expression. D) mRNA and E) protein expression of CHAC1 in thyroid carcinoma cell lines, K1, BCPAP, and TPC1 cells, and a normal human thyroid follicular epithelial cell line, Nthy-ori3-1. **p<0.01, ***p<0.001 vs. normal or Nthy-ori3-1

cantly suppressed cell viability in BCPAP cells (Figure 2C). We then explored how CHAC1 overexpression exerted the inhibition effects on thyroid carcinoma cells. BCPAP cells overexpressing CHAC1 were exposed to ferroptosis inhibitor Fer-1 [21], apoptosis inhibitor Z-VAD-FMK [22], or autophagy inhibitor 3-MA [23] for 48 h. As shown in Figure 2D, CHAC1 overexpression significantly inhibited cell viability, which was abolished by Fer-1, but not by Z-VAD-FMK or 3-MA. These data indicated that ferroptosis may be involved in the viability inhibition effects of CHAC1 overexpression in thyroid carcinoma cells.

We then detected lipid ROS production and expression of two ferroptosis markers GPX4 and PTGS2 [24, 25] in BCPAP cells overexpressing CHAC1. In CHAC1-overex-

pressing BCPAP cells, lipid ROS production was increased as compared to Vector cells (Figure 2E). GPX4 protein expression was decreased, while PTGS2 protein expression was increased in CHAC1-overexpressing BCPAP cells (Figure 2F). These data suggest that overexpression of CHAC1 inhibited cell viability and promoted ferroptosis in thyroid carcinoma.

Overexpression of CHAC1 inhibited tumor growth in thyroid carcinoma *in vivo*. Next, we wondered whether the effects of CHAC1 overexpression exist *in vivo*, so xenograft experiments were performed. Nude mice were subcutaneously injected with BCPAP cells transfected with CHAC1 expressing vector or blank vector, and tumor volumes were measured every three days till day 35. A slower growth rate was observed in tumors formed from the CHAC1-overexpressing cells as compared with that in the control group (Figure 3A). Tumor size and weight were also significantly reduced in the CHAC1 overexpression group on day 35 (Figures 3B, 3C). To explore whether the slower tumor growth was ascribed to decreased proliferation, we performed an immunofluorescence staining with anti-Ki-67. Our results showed that Ki-67-positive cells were reduced in the CHAC1 overexpression group compared to the control group (Figures 3D, 3E). Moreover, GPX4 protein expression was decreased, while CHAC1 and PTGS2 protein expressions were increased in xenografts injected with CHAC1-overexpressing cells (Figure 3F).

CHAC1 knockdown promoted cell viability in thyroid carcinoma via inhibiting ferroptosis. To further investigate the involvement of ferroptosis in the functions of CHAC1, CHAC1 was knocked down in K1 cells, and then treated with or without RSL3, a ferroptosis inducer. As shown in Figures 4A and 4B, three shRNA targeting CHAC1 notably suppressed its mRNA and protein expression in K1 cells. Knocking down of CHAC1 significantly promoted cell viability, which was attenuated by RSL3 treatment (Figure 4C). K1 cells with CHAC1 knockdown showed reduced lipid ROS production (Figure 4D) and PTGS2 protein expression, and enhanced GPX4 protein expression (Figure 4E), which were also abolished by RSL3 exposure. These findings indicated ferroptosis mediated the inhibiting role of CHAC1 in thyroid carcinoma cell viability.

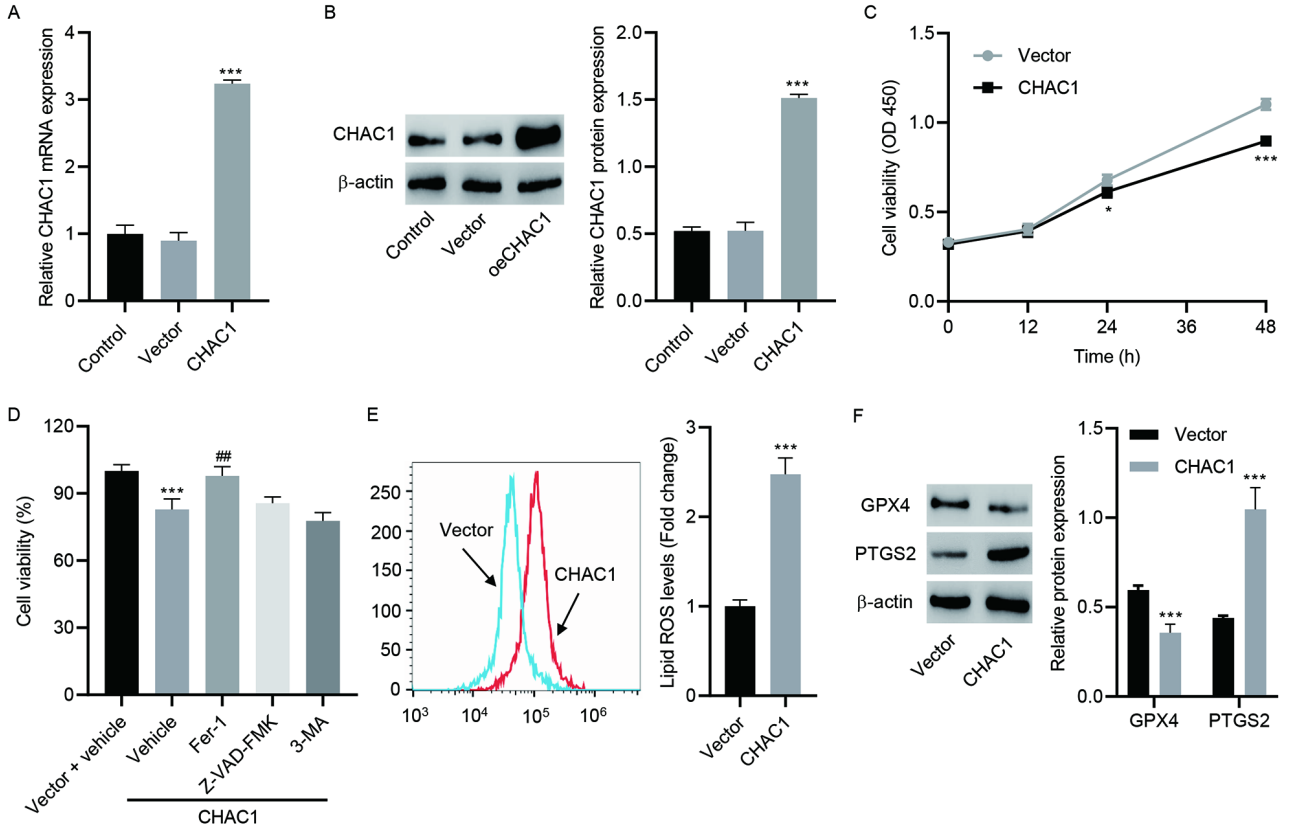

Figure 2. Overexpression of CHAC1 inhibited the cell viability and promoted ferroptosis in thyroid carcinoma. A) mRNA and B) protein expression of CHAC1 in BCPAP cells transfected with CHAC1 expression vector or blank vector. C) Cell Counting Kit-8 (CCK-8) assays were performed to evaluate BCPAP cell viability. D) BCPAP cells overexpressing CHAC1 were treated with 5 mM Fer-1, 10 mM Z-VAD-FMK, 5 mM 3-MA or vehicle (DMSO), and cell viability was detected by CCK-8 assays at 48 h. E) Lipid ROS was detected by flow cytometry. F) GPX4 and PTGS2 expression was detected by western blotting. *p<0.05, ***p<0.001 vs. vector or vector+vehicle; ##p<0.01 vs. CHAC1+vehicle

CHAC1 affected radiation sensitivity in thyroid carcinoma cells. We then examined whether CHAC1 affected radiation sensitivity in thyroid carcinoma cells. As shown in Figure 5A, the cell viability of BCPAP cells and K1 cells was dose-dependently decreased by radiation. The viability of BCPAP and K1 cells was > 70% in the presence of 4 Gy of radiation, thus 4 Gy was chosen for the following experiments. The viability of BCPAP cells induced by 4 Gy of

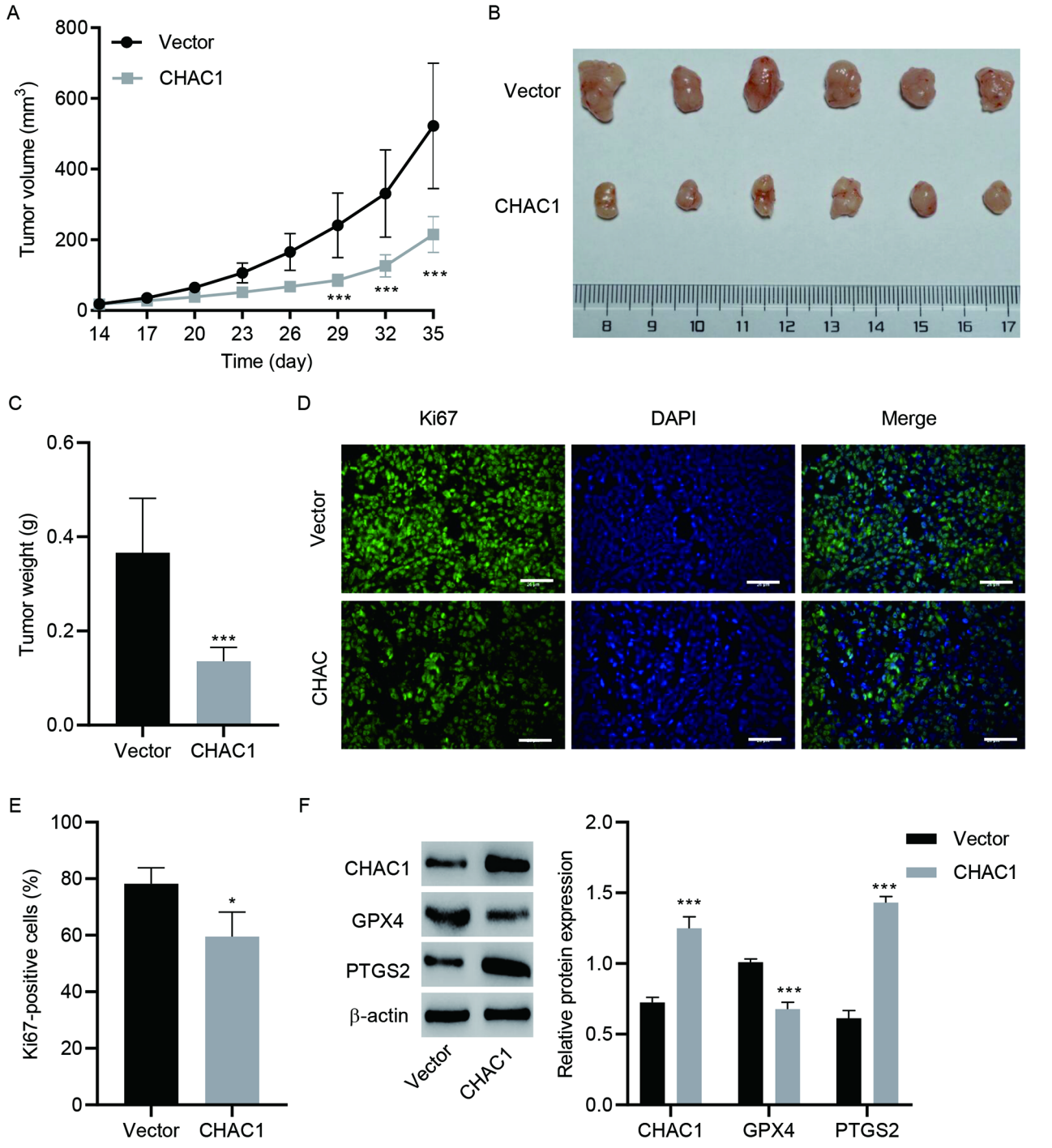

Figure 3. Overexpression of CHAC1 inhibited tumor growth *in vivo*. Nude mice were subcutaneously injected with BCPAP cells transfected with CHAC1 expression vector or blank vector. A) Tumor volume was recorded every three days. After 35 days, B) the xenografts were photographed, and C) the tumor weights were examined, and then processed by D) immunofluorescence staining with anti-Ki67 and E) quantitated. Scale bar, 100 mm. F) GPX4 and PTGS2 expression was detected by western blotting. *p<0.05, ***p<0.001 vs. vector

radiation was further decreased by CHAC1 overexpression (Figure 5B). On the contrary, the viability of K1 cells induced by 4 Gy of radiation was increased by CHAC1 knocking down (Figure 5C). Moreover, the viability of BCPAP cells induced by 4 Gy of radiation and CHAC1 overexpression was increased by Fer-1 (Figure 5D). These data suggested that CHAC1 overexpression enhanced radiation sensitivity in thyroid carcinoma cells, while CHAC1 knockdown had reversed effects.

Discussion

Although studies have reported that CHAC1 expression was closely related to various types of cancers [15, 16, 18], few studies have investigated the effects of CHAC1 expression on patients with thyroid carcinoma. In the current study, we first revealed the lower expression of CHAC1 in both thyroid carcinoma tissues and cell lines, and that low CHAC1 expression was negatively correlated with TNM stage and tumor size. We also provided evidence for the role of CHAC1 in regulating the viability and radiation sensitivity of thyroid carcinoma cells and proposed that CHAC1-induced ferroptosis may mediate its role in cell viability inhibition.

Ferroptosis has attracted much attention in cancer and cancer treatment since Dixon et al. reported that erastin induced ferroptosis in RAS mutant tumor cell lines [10]. Multiple ferroptosis regulators, such as p53, HO-1, and p62-Keap1-NRF2, are found to be associated with cancer progression [6, 26]. For example, ferroptosis was found to mediate the tumor suppressive function of p53. p53 sensitizes cells to ferroptosis by transcriptional suppression of cystine transporter SLC7A11, thus rendering cancer cells more resistant to ferroptosis [27]. Furthermore, accumulated evidence has proposed the potential of ferroptosis as an anti-cancer therapy. Some drugs or compounds have been found to induce ferroptosis of tumor cells. Several ferroptosis inducers could efficiently suppress tumor growth in various experimental cancer models [28]. It has been reported that CHAC1 overexpression led to intracellular glutathione depletion and increased ROS levels [7, 8], taking part in the process of ferroptosis. In the current study, we found that the viability of thyroid carcinoma cells overexpressing CHAC1 was increased by a ferroptosis inhibitor, but not an apoptosis inhibitor or an autophagy inhibitor, indicating the involvement of ferroptosis. Following experiments with CHAC1-knockdown cells exposed to a ferroptosis inducer

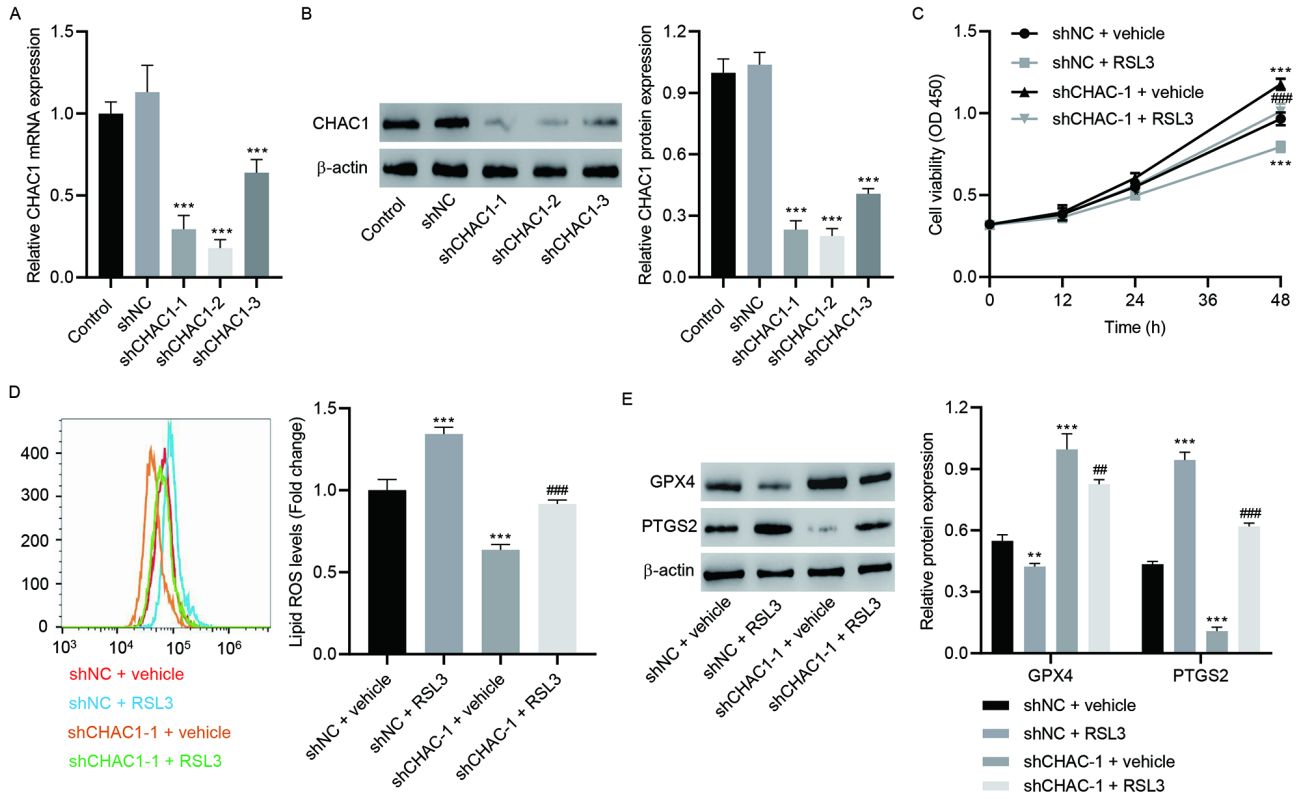

Figure 4. CHAC1 knockdown promoted BCPAP cell viability by inhibiting ferroptosis. A) mRNA and B) protein expression of CHAC1 in K1 cells transduced with CHAC1 shRNA vector or control shRNA (shNC) vector. K1 cells with CHAC1 knockdown were treated with 1 mg/mL RSL3 and C) cell viability, D) lipid ROS, E) GPX4 and PTGS2 expression were detected by CCK-8, flow cytometry, and western blotting, respectively. ***p<0.001 vs. shNC or shNC+vehicle; ##p<0.01, ###p<0.001 vs. shCHAC1+vehicle

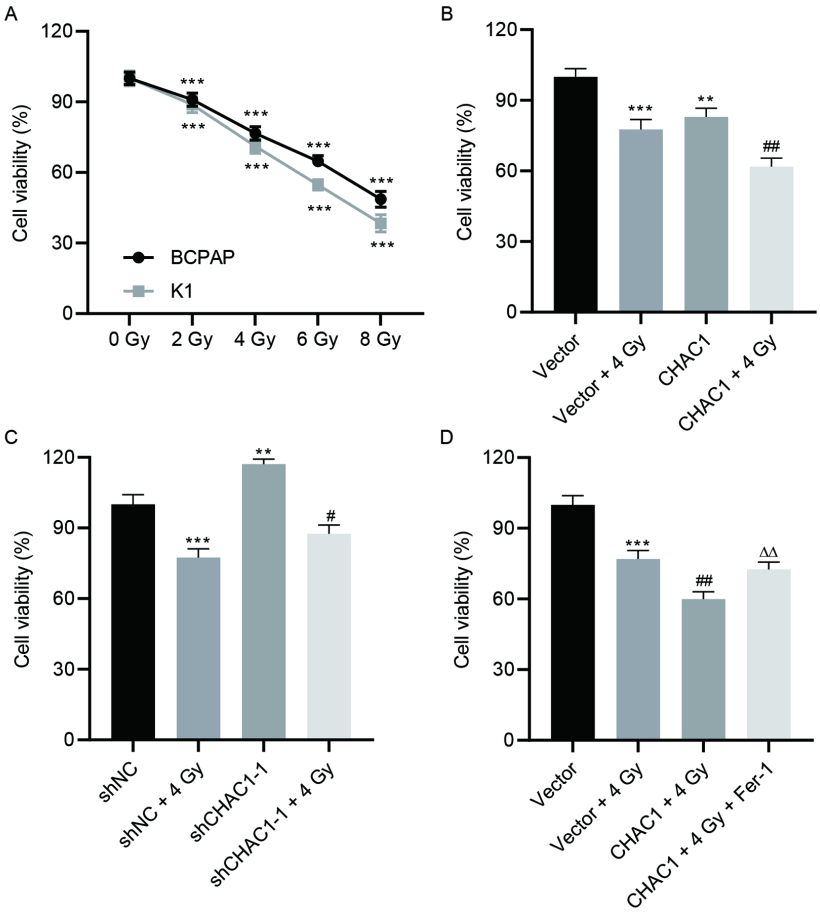

Figure 5. CHAC1 affected thyroid carcinoma cells' response to radiation. A) BCPAP and K1 cells were exposed to radiation (0, 2, 4, 6, and 8Gy), and cell viability was detected by CCK-8 assay at 48 h. B) BCPAP cells overexpressing CHAC1 were exposed to radiation (4 Gy), and cell viability was detected by CCK-8 assay at 48 h. C) K1 cells with CHAC1 knockdown were exposed to radiation (4 Gy), and cell viability was detected by CCK-8 assay at 48 h. D) BCPAP cells overexpressing CHAC1 were exposed to radiation (4 Gy) with or without 5 mM Fer-1 treatment, and cell viability was detected by CCK-8 assay at 48 h. **p<0.01, ***p<0.001 vs. 0 Gy, vector or shNC; #p<0.05, ##p<0.01 vs. vector+4 Gy or shNC+4 Gy; ΔΔp<0.01 vs. CHAC1+4 Gy

further confirmed that ferroptosis may mediate the viability inhibition effect of CHAC1 in thyroid carcinoma cells. In a word, CHAC1 overexpression could induce ferroptosis, thus playing a suppressive function in thyroid carcinoma cells.

GPX4 can protect cells against lipid peroxidation by its antioxidant activity. Knockout of the GPX4 gene in mice resulted in embryonic lethality and lipid peroxides accumulation [29]. Further analysis suggested that ferroptosis but not apoptosis was the leading cause of the lethality [30]. Elevated expression of GPX4 has been found in a variety of cancers, such as gastric cancer [31], esophageal carcinoma [32], and thyroid carcinoma [33]. Bioinformatics analysis showed that high mRNA expression of GPX4 was found in thyroid carcinoma tissues and associated with a favorable prognosis (Supplementary Figures S1C, S1D). Additionally, we found that CHAC1 protein expression was negatively correlated with GPX4 protein expression in thyroid carcinoma tissues and cells, which was consistent with the previous study [14]. Moreover, correlation analysis showed that CHAC1 mRNA expression was negatively correlated with GPX4 mRNA expression in thyroid carcinoma tissues in the GEPIA database (Supplementary Figure S1G). Furthermore, ferroptosis inducer RSL3, an inhibitor of GPX4 [34], also inhibited CHAC1 knockdown-mediated cell viability and ferroptosis, suggesting that CHAC1 may exert functions through regulating GPX4.

High PTGS2 protein expression in papillary thyroid carcinoma is associated with adverse survival outcomes [35]. However, our bioinformatics analysis showed that the mRNA expression of PTGS2 in normal and tumor tissues was similar, and PTGS2 mRNA expression was not prognostic in thyroid carcinoma (Supplementary Figures S1E, S1F). These data suggested that the prognostic value of PTGS2 in thyroid carcinoma may be dependent on different transcriptional and translational regulations of PTGS2 and tumor histologies. Additionally, we found that CHAC1 protein expression

was positively correlated with PTGS2 protein expression in thyroid carcinoma cells. However, CHAC1 mRNA expression was negatively correlated with PTGS2 mRNA expression in thyroid carcinoma tissues in the GEPIA database (Supplementary Figure S1H). Therefore, further experiments are required to validate the regulatory mechanism of PTGS2 expression by CHAC1 in thyroid carcinoma.

Radiotherapy is one of the main methods of thyroid carcinoma treatment [5]. In the current study, the data suggested that CHAC1 overexpression was able to enhance the radiation sensitivity of thyroid carcinoma cells and *vice versa*. Further experiments using animal models or clinical samples are required to validate the effects of CHAC1 on radiotherapy sensitivity.

In conclusion, CHAC1 suppressed thyroid carcinoma cells *in vitro* and *in vivo*, and enhanced cell sensitivity to radiation. CHAC1-induced ferroptosis may mediate its role in thyroid carcinoma cells. This study might provide a theoretical basis for the prevention and treatment of thyroid carcinoma.

Supplementary information is available in the online version of the paper.

Acknowledgments: This study was supported by grants from Special Disease Construction of Pudong Health Bureau of Shanghai (PWZzb2022-02), Shanghai Municipal Health Committee (20204Y0170, 201840338), Shanghai Pudong Science and Technology Committee (PKJ2021-Y04), Shanghai Science and Technology Committee (20S21901900) and the Project of Shanghai Pudong National Pilot Zone for Comprehensive Reform of Traditional Chinese Medicine Development (PDZY-2019-0807).

References

[1] FILETTI S, DURANTE C, HARTL D, LEBOULLEUX S, LOCATI LD et al. Thyroid cancer: ESMO Clinical Practice Guidelines for diagnosis, treatment and follow-updagger. Ann Oncol 2019; 30: 1856–1883. https://doi.org/10.1093/annonc/mdz400

[2] ALONSO-GORDOA T, DÍEZ JJ, DURÁN M, GRANDE E. Advances in thyroid cancer treatment: latest evidence and clinical potential. Ther Adv Med Oncol 2015; 7: 22–38. https://doi.org/10.1177/1758834014551936

[3] SANABRIA A, KOWALSKI LP, SHAH JP, NIXON IJ, ANGELOS P et al. Growing incidence of thyroid carcinoma in recent years: Factors underlying overdiagnosis. Head Neck 2018; 40: 855–866. https://doi.org/10.1002/hed.25029

[4] HU J, YUAN IJ, MIRSHAHIDI S, SIMENTAL A, LEE SC et al. Thyroid Carcinoma: Phenotypic Features, Underlying Biology and Potential Relevance for Targeting Therapy. Int J Mol Sci 2021; 22: 1950. https://doi.org/10.3390/ijms22041950

[5] KITAHARA CM, SOSA JA. The changing incidence of thyroid cancer. Nat Rev Endocrinol 2016; 12: 646–653. https://doi.org/10.1038/nrendo.2016.110

[6] DIXON SJ, STOCKWELL BR. The Hallmarks of Ferroptosis. Ann Rev Cancer Biol 2019; 3: 35. https://doi.org/10.1146/annurev-cancerbio-030518-055844

[7] DIXON SJ, STOCKWELL BR. The role of iron and reactive oxygen species in cell death. Nat Chem Biol 2014; 10: 9–17. https://doi.org/10.1038/nchembio.1416

[8] D'HERDE K, KRYSKO DV. Ferroptosis: Oxidized PEs trigger death. Nat Chem Biol 2017; 13: 4–5. https://doi.org/10.1038/nchembio.2261

[9] GAO M, MONIAN P, QUADRI N, RAMASAMY R, JIANG X. Glutaminolysis and Transferrin Regulate Ferroptosis. Mol Cell 2015; 59: 298–308. https://doi.org/10.1016/j.molcel.2015.06.011

[10] DIXON SJ, LEMBERG KM, LAMPRECHT MR, SKOUTA R, ZAITSEV EM et al. Ferroptosis: an iron-dependent form of nonapoptotic cell death. Cell 2012; 149: 1060–1072. https://doi.org/10.1016/j.cell.2012.03.042

[11] KUMAR A, TIKOO S, MAITY S, SENGUPTA S, SENGUPTA S et al. Mammalian proapoptotic factor ChaC1 and its homologues function as γ-glutamyl cyclotransferases acting specifically on glutathione. EMBO Rep 2012; 13: 1095–1101. https://doi.org/10.1038/embor.2012.156

[12] CRAWFORD RR, PRESCOTT ET, SYLVESTER CF, HIGDON AN, SHAN J et al. Human CHAC1 Protein Degrades Glutathione, and mRNA Induction Is Regulated by the Transcription Factors ATF4 and ATF3 and a Bipartite ATF/CRE Regulatory Element. J Biol Chem 2015; 290: 15878–15891. https://doi.org/10.1074/jbc.M114.635144

[13] CRAWFORD RR, PRESCOTT ET, MUNGRUE IN. Genetic Inhibition of Chac1 Leads to Dysregulation of Body Composition. FASEB J 2016; 30. https://doi.org/10.1096/fasebj.30.1_supplement.717.3

[14] HE S, ZHANG M, YE Y, ZHUANG J, MA X et al. ChaC glutathione specific γ-glutamylcyclotransferase 1 inhibits cell viability and increases the sensitivity of prostate cancer cells to docetaxel by inducing endoplasmic reticulum stress and ferroptosis. Exp Ther Med 2021; 22: 997. https://doi.org/10.3892/etm.2021.10429

[15] MEHTA V, MEENA J, KASANA H, MUNSHI A, CHANDER H. Prognostic significance of CHAC1 expression in breast cancer. Mol Biol Rep 2022; 49: 8517–8526. https://doi.org/10.1007/s11033-022-07673-x

[16] GOEBEL G, BERGER R, STRASAK AM, EGLE D, MÜLLER-HOLZNER E et al. Elevated mRNA expression of CHAC1 splicing variants is associated with poor outcome for breast and ovarian cancer patients. Br J Cancer 2012; 106: 189–198. https://doi.org/10.1038/bjc.2011.510

[17] CHEN MS, WANG SF, HSU CY, YIN PH, YEH TS et al. CHAC1 degradation of glutathione enhances cystine-starvation-induced necroptosis and ferroptosis in human triple negative breast cancer cells via the GCN2-eIF2α-ATF4 pathway. Oncotarget 2017; 8: 114588–114602. https://doi.org/10.18632/oncotarget.23055

[18] CHEN PH, SHEN WL, SHIH CM, HO KH, CHENG CH et al. The CHAC1-inhibited Notch3 pathway is involved in temozolomide-induced glioma cytotoxicity. Neuropharmacology 2017; 116: 300–314. https://doi.org/10.1016/j.neuropharm.2016.12.011

[19] JOO NE, RITCHIE K, KAMARAJAN P, MIAO D, KAPILA YL. Nisin, an apoptogenic bacteriocin and food preservative, attenuates HNSCC tumorigenesis via CHAC1. Cancer Med 2012; 1: 295–305. https://doi.org/10.1002/cam4.35

[20] ZHANG Y, ZHOU X, CHENG X, HONG X, JIANG X et al. PRKAA1, stabilized by FTO in an m6A-YTHDF2-dependent manner, promotes cell proliferation and glycolysis of gastric cancer by regulating the redox balance. Neoplasma 2022; 69: 1338–1348. https://doi.org/10.4149/neo_2022_220714N714

[21] LIU P, FENG Y, LI H, CHEN X, WANG G et al. Ferrostatin-1 alleviates lipopolysaccharide-induced acute lung injury via inhibiting ferroptosis. Cell Mol Biol Lett 2020; 25: 10. https://doi.org/10.1186/s11658-020-00205-0

[22] LAN W, SANTOFIMIA-CASTAÑO P, XIA Y, ZHOU Z, HUANG C et al. Targeting NUPR1 with the small compound ZZW-115 is an efficient strategy to treat hepatocellular carcinoma. Cancer Lett 2020; 486: 8–17. https://doi.org/10.1016/j.canlet.2020.04.024

[23] ZHAO D, WANG W, WANG H, PENG H, LIU X et al. PKD knockdown inhibits pressure overload-induced cardiac hypertrophy by promoting autophagy via AKT/mTOR pathway. Int J Biol Sci 2017; 13: 276–285. https://doi.org/10.7150/ijbs.17617

[24] CHEN G, LI L, TAO H. Bioinformatics Identification of Ferroptosis-Related Biomarkers and Therapeutic Compounds in Ischemic Stroke. Front Neurol 2021; 12: 745240. https://doi.org/10.3389/fneur.2021.745240

[25] LIU L, YANG S, WANG H. α-Lipoic acid alleviates ferroptosis in the MPP+ -induced PC12 cells via activating the PI3K/Akt/Nrf2 pathway. Cell Biol Int 2021; 45: 422–431. https://doi.org/10.1002/cbin.11505

[26] XU T, DING W, JI X, AO X, LIU Y et al. Molecular mechanisms of ferroptosis and its role in cancer therapy. J Cell Mol Med 2019; 23: 4900–4912. https://doi.org/10.1111/jcmm.14511

[27] JIANG L, KON N, LI T, WANG SJ, SU T et al. Ferroptosis as a p53-mediated activity during tumour suppression. Nature 2015; 520: 57–62. https://doi.org/10.1038/nature14344

[28] HASSANNIA B, VANDENABEELE P, BERGHE TV. Targeting ferroptosis to iron out cancer. Cancer Cell 2019; 35: 830–849. https://doi.org/10.1016/j.ccell.2019.04.002

[29] YOO SE, CHEN L, NA R, LIU Y, RIOS C et al. Gpx4 ablation in adult mice results in a lethal phenotype accompanied by neuronal loss in brain. Free Radic Biol Med 2012; 52: 1820–1827. https://doi.org/10.1016/j.freeradbiomed.2012.02.043

[30] SEILER A, SCHNEIDER M, FÖRSTER H, ROTH S, WIRTH EK et al. Glutathione peroxidase 4 senses and translates oxidative stress into 12/15-lipoxygenase dependent- and AIF-mediated cell death. Cell Metab 2008; 8: 237–248. https://doi.org/10.1016/j.cmet.2008.07.005

[31] LI D, WANG Y, DONG C, CHEN T, DONG A et al. CST1 inhibits ferroptosis and promotes gastric cancer metastasis by regulating GPX4 protein stability via OTUB1. Oncogene 2023; 42: 83–98. https://doi.org/10.1038/s41388-022-02537-x

[32] POHL SÖ, PERVAIZ S, DHARMARAJAN A, AGOSTINO M. Gene expression analysis of heat-shock proteins and redox regulators reveals combinatorial prognostic markers in carcinomas of the gastrointestinal tract. Redox Biol 2019; 25: 101060. https://doi.org/10.1016/j.redox.2018.11.018

[33] SEKHAR KR, HANNA DN, CYR S, BAECHLE JJ, KURAVI S et al. Glutathione peroxidase 4 inhibition induces ferroptosis and mTOR pathway suppression in thyroid cancer. Sci Rep 2022; 12: 19396. https://doi.org/10.1038/s41598-022-23906-2

[34] BAOYINNA B, MIAO J, OLIVER PJ, YE Q, SHAHEEN N et al. Non-Lethal Doses of RSL3 Impair Microvascular Endothelial Barrier through Degradation of Sphingosie-1-Phosphate Receptor 1 and Cytoskeletal Arrangement in A Ferroptosis-Independent Manner. Biomedicines 2023; 11: 2451. https://doi.org/10.3390/biomedicines11092451

[35] AL-MAGHRABI JA, GOMAA W. High COX-2 immunostaining in papillary thyroid carcinoma is associated with adverse survival outcomes. Ann Saudi Med 2022; 42: 359–365. https://doi.org/10.5144/0256-4947.2022.359

https://doi.org/10.4149/neo_2023_230103N4

CHAC1 promotes cell ferroptosis and enhances radiation sensitivity in thyroid carcinoma

Xinlin YANG[1,#], Miao ZHANG[2,#], Wei XIA[1], Zhongchao MAI[1], Ying YE[2], Bin ZHAO[3,*], Yanan SONG[2,*]

Supplementary Information

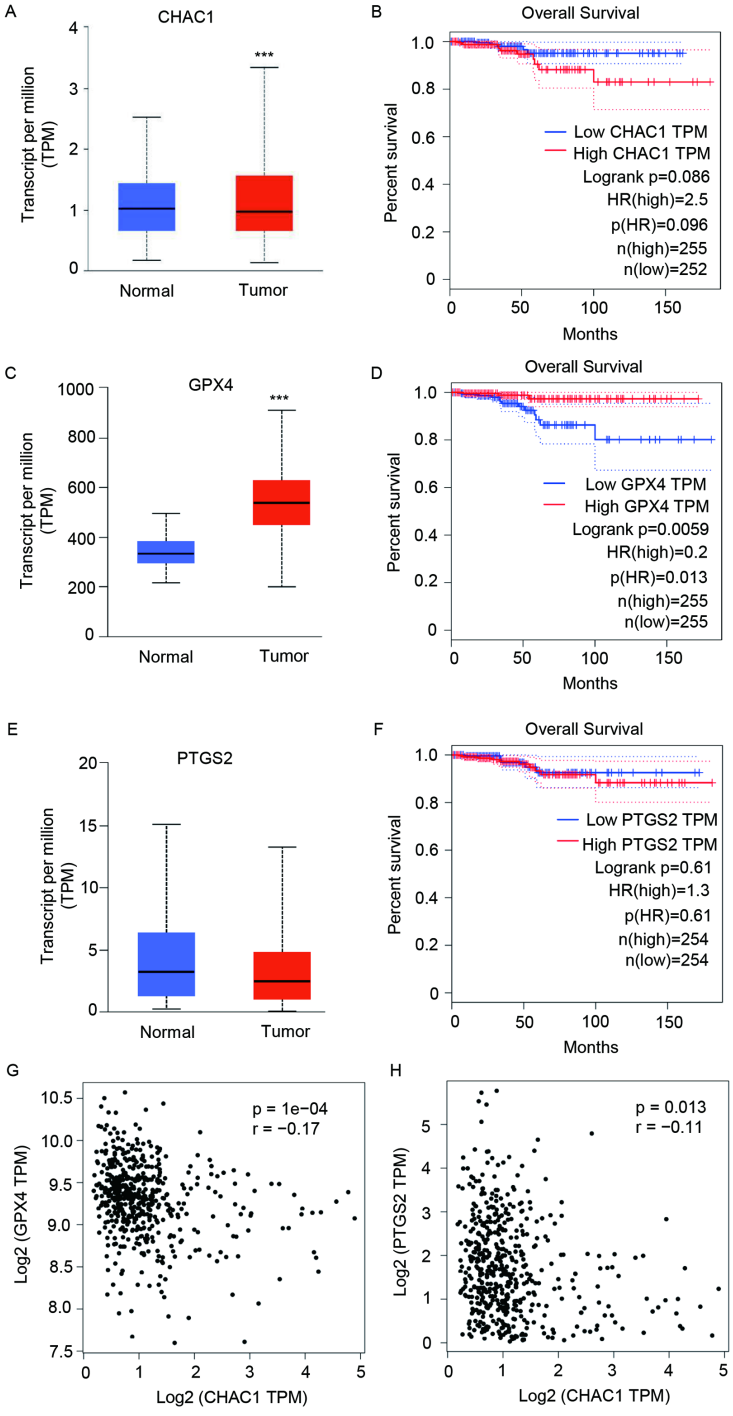

Supplementary Figure S1. A) Comparison of CHAC1 expression in thyroid carcinoma tissues with normal thyroid tissues in UALCAN database; B) Correlation of CHAC1 mRNA expression with prognosis of patients with thyroid carcinoma showed by GEPIA; C, D) Bioinformatics analysis of mRNA expression of GPX4 in thyroid carcinoma tissues; G) GEPIA database correlation analyses of CHAC1 mRNA expression and GPX4 mRNA expression in thyroid carcinoma tissues; E, F) Bioinformatics analysis of mRNA expression of PTGS2 in normal and tumor tissues; H) GEPIA database correlation of Chac1 mRNA expression and PTGS2 mRNA expression in thyroid carcinoma tissues